SLAC-PUB-10385

# *In-situ* Grazing-Incidence EXAFS Study of Pb(II) Chemisorption on Hematite (0001) and (1-102) Surfaces

*John R. Bargar[1*], Thomas P. Trainor[2†], Jeffery P. Fitts[2††], Scott A. Chambers[3], and Gordon E. Brown, Jr.[1,2]*

[1]Stanford Synchrotron Radiation Laboratory, SLAC, 2575 Sand Hill Road, MS 69, Menlo Park, CA 94025, USA

[2]Surface & Aqueous Geochemistry Group, Department of Geological & Environmental Sciences, Stanford University, Stanford, CA 94305-2115, USA

[3]Environmental Molecular Sciences Laboratory, Pacific Northwest National Laboratory, 908 Battelle Boulevard, Richland, WA 99352, USA

[†]Present Address: Department of Chemistry and Biochemistry, University of Alaska, Fairbanks, Fairbanks, AK. [††]Present Address: Department of Environmental Sciences, Brookhaven National Laboratory, Upton, NY, USA

REVISED MANUSCRIPT SUBMITTED October 30, 2003

*Corresponding author. Phone: (650-926-4949), Fax: (650)-926-4100, e-mail: bargar@slac.stanford.edu.

*Work supported in part by the Department of Energy contract DE-AC03-76SF00515.*

## ABSTRACT

The dominant mode of binding of aqueous Pb(II) to single crystal (0001) (C-cut) and (1-102) (R-cut) surfaces of $\alpha$-$Fe_2O_3$ has been determined using grazing-incidence x-ray absorption fine structure (GI-XAFS) spectroscopy. Oligomeric Pb(II) complexes were found to bind in inner-sphere modes on both surfaces, which is in contrast with the binding of aqueous Pb(II) on $\alpha$-$Al_2O_3$ (0001) surfaces, where Pb(II) was found in past GI-XAFS studies to bind in a dominantly outer-sphere mode, indicating a significant difference in reactivity of these two surfaces to Pb(II). This difference in reactivity to Pb(II) is explained on the basis of recent crystal truncation rod diffraction studies of the $\alpha$-$Fe_2O_3$ and $\alpha$-$Al_2O_3$ C-cut surfaces in contact with bulk water, which found major structural differences between the surfaces of these two metal oxides.

## Introduction

Heavy metal ion transport in natural waters is influenced by reactions between solute species and solid materials (*e.g.*, mineral surfaces, humic materials, biomass).[1] Adsorption of cations onto mineral surfaces is of major importance for heavy metal attenuation, even in biomass-rich systems.[2,3] In particular, Fe- and Mn-oxides and (oxy)hydroxides are very common in the environment and have high sorptive capacities for metal ions in the pH ranges of most natural waters. The reactivity of a metal-oxide surface is controlled, in part, by the types and concentrations of surface sites exposed to aqueous solution.[4] In addition, surface site reactivity is key to heterogeneous chemical processes such as catalysis, crystal growth, preparation of semiconductors, and energy storage in fuel cells.[1] Little is known at present about the structure and composition of reactive sites on metal-oxide surfaces in contact with aqueous solutions, due largely to the difficulty of probing such sites experimentally. In the present study, the structures of Pb(II) complexes adsorbed on two common hematite ($\alpha$-$Fe_2O_3$) single crystal surfaces [(0001) (C-cut) and (1-102) (R-cut)] were studied using grazing incidence x-ray absorption fine structure (XAFS) spectroscopy under *in-situ* conditions (*i.e.*, in the presence of bulk solution at ambient temperature and pressure) in order to obtain information on reactive surface sites to which Pb(II) preferentially binds as well as information on the structure and composition of the Pb(II) surface complexes.

Several general models have been advanced in recent years to relate macroscopic uptake data for metal ions to the structures and compositions of individual surface sites on metal oxides and (oxy)hydroxides.[7-14] With respect to hematite, Bargar *et al.*[7] predicted that Pb(II) should not react strongly with the $\alpha$-$Fe_2O$ C-cut surface, based on bond valence considerations of ideal surface oxygen coordination environments (*i.e.,* $\equiv Fe_2O$) (see Fig. 1) and the fact that Pb(II) was observed to form dominantly outer-sphere complexes on the hydrated $\alpha$-$Al_2O_3$ C-cut surface (*i.e.*, maintained in contact with saturated humid atmosphere after reaction with Pb(II) in bulk solution). In contrast, the binding of

Pb(II) to the R-cut surfaces of $\alpha$-$Fe_2O_3$ and $\alpha$-$Al_2O_3$ is predicted to be relatively strong because Pb(II) should readily bond to $\equiv FeO$ and $\equiv Fe_3O$ groups on hematite as well as to $\equiv AlO$ and $\equiv Al_3O$ surface groups on $\alpha$-alumina[8] both of which are thought to be prevalent on the R-cut surfaces. Subsequently, Ostergren *et al.*[9] proposed a modified bond valence model in which limited surface relaxation was considered. That study concluded that Pb(II) should bond to $\equiv Fe_2O$ surface groups if the Fe-O bonds lengthen significantly from their bulk values. In both cases, the models emphasize bonding of metal ions to surface oxygens and generally do not account for geometric factors such as the O-O distances on oxide surfaces, where bidentate bonding of metal ion complexes may occur. These models also do not account for non-ideal surface stoichiometries and structures (the structural details of which are often unknown), which may result from hydration of the crystallographic terminations of the bulk crystals. A measure of the relative reactivity of $\alpha$-$Al_2O_3$ and $\alpha$-$Fe_2O_3$ surfaces for Pb(II) comes from the X-ray standing wave study of Templeton *et al.*[3] who determined Pb(II) uptake on the hematite C-cut surface and the $\alpha$-$Al_2O_3$ C- and R-cut surfaces and showed that their reactivities with respect to Pb(II) under the experimental conditions of that study follow the order: hematite C-cut > $\alpha$-$Al_2O_3$ R-cut > $\alpha$-$Al_2O_3$ C-cut. These results further suggest that Pb(II) binding modes and compositions of surface functional groups on these surfaces are not the same.

Testing these model predictions and understanding the observed behavior of Pb(II) on different surfaces of these metal oxides requires a surface-sensitive structural probe that can provide local structural information about the sorbate at low adsorption densities ($\leq 1$ $\mu$mol/m$^2$ or $\leq 0.03$ monolayers, based on an ideal oxygen site density of 36.4 $\mu$moles/m$^2$), interacting with specific oxide surface sites, under *in-situ* conditions. Grazing incidence (GI-) EXAFS spectroscopy provides these capabilities when used to study metal ions adsorbed on surfaces of oriented single-crystal samples.[7,8,13,14]

In the present study we have used GI-EXAFS spectroscopy to investigate the reactivity of hematite C- and R-cut surfaces in direct contact with aqueous solution containing Pb(II). Pb(II) was chosen as the sorbate because of its importance as a major heavy metal pollutant in soils, mining wastes, and aquatic ecosystems[15] and the fact that there have been a number of EXAFS studies of Pb(II) sorption complexes on single crystal $\alpha$-alumina surfaces[7,8] and on high surface area Fe- and Al-(oxyhydr)oxides[16], with which our results can be compared. Hematite was chosen as the sorbent because it is a common phase in soils and sediments, and the structure of the hydrated C-cut hematite surface has recently been studied under *in-situ* conditions by both STM[17] and crystal truncation rod diffraction studies,[18,19] which provide a basis for understanding the differences in reactivity of the $\alpha$-$Fe_2O_3$ and $\alpha$-$Al_2O_3$ single crystal surfaces. As discussed below, Pb(II) was found to adsorb as inner-sphere complexes on both of these surfaces. This result is discussed in the context of surface structural models.

## Surface Structure and Reactivity of Hematite (0001) and (1-102)

The idealized structures of the oxygen-terminated hematite C-cut and R-cut surfaces are illustrated in Figure 1. An important question in the context of the present study is whether or not the ideal oxygen-terminated C- and R-cut surfaces of hematite are representative of these surfaces in the presence of bulk water, which are the relevant concern in natural systems. Oxygen 1s photoemission measurements of the hematite C-cut surface before and after exposure to water vapor at pressures ranging from $10^{-8}$ Torr to 1 Torr (3 min. exposure times at each pressure), showed that the C-cut surface undergoes significant hydroxylation (> 0.5 monolayer) at a "threshold" pressure of $\approx 3 \times 10^{-4}$ Torr for an exposure time of 3 min. ($1.8 \times 10^4$ L).[20] A similar study of the presumably isostructural $\alpha$-$Al_2O_3$ C-cut surface revealed a "threshold" pressure for significant hydroxylation of 1 Torr.[20] These results indicate that the two surfaces do not have similar reactivities to water and suggest that they may not have similar structures.

Previous STM studies,[21-23] LEED studies,[23,24] and spin density functional calculations,[22] provide evidence for both O- and Fe-terminations on the hematite C-cut surface under ultra-high vacuum and surface preparations. We are aware of only two studies of the surface structure of the hydrated hematite C-cut surface under ambient temperature/pressure conditions with bulk water present, one involving

STM imaging[17] and one involving crystal truncation rod (CTR) diffraction.[18,19] The *in-situ* STM images of the C-cut hematite surface from the study of Eggleston *et al.*[17] were interpreted as indicating a multi domain surface and that the observed domains are chemically distinct, consisting of oxygen terminated regions and regions with Fe(III) present in an adsorbed state.

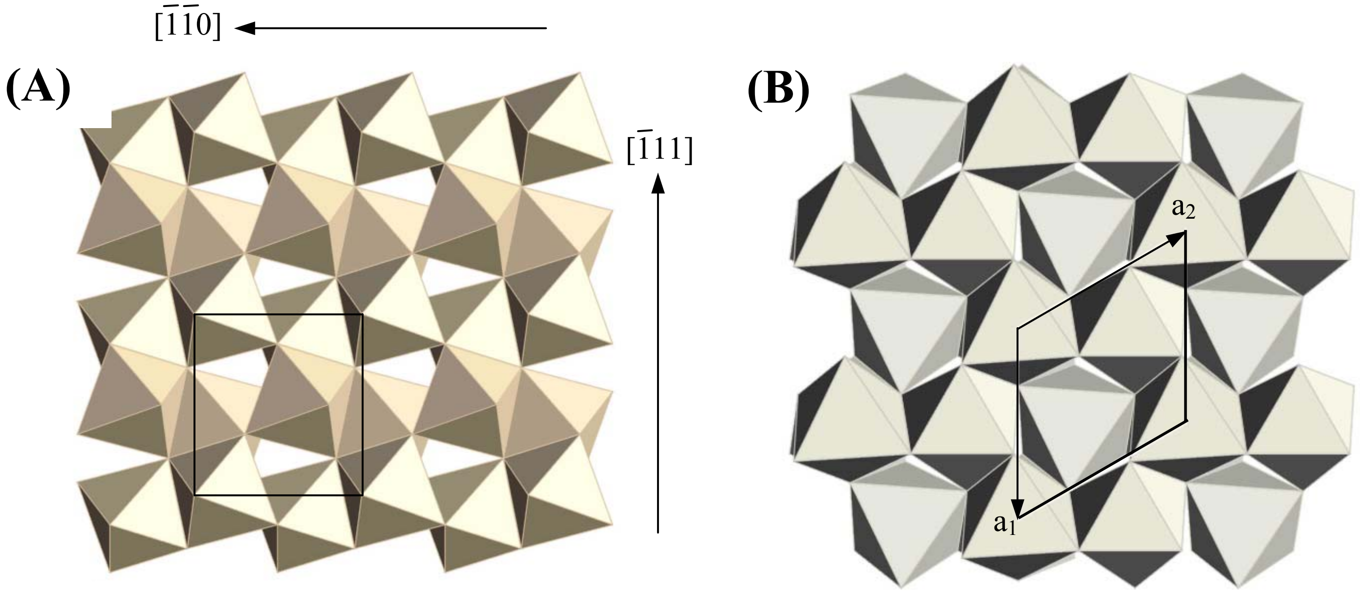

**Figure 1.** (A) Polyhedral representation of the oxygen-terminated R-cut surface. Surface unit cell is outlined in black. Surface unit cell edge lengths are 5.038 Å for the edge parallel to [110] and 5.435 Å for the edge parallel to [111] (c-axis projection). (B) Polyhedral representation of the oxygen-terminated hematite C-cut surface. Unit cell edge-length is 5.038 Å.

The CTR x-ray diffraction study of the hydrated hematite C-cut surface by Trainor et al.[18,19] found evidence for substantial relaxation of the top three layers of the C-cut surface. The most important finding regarding surface reactivity is that the hydrated hematite C-cut surface is oxygen (or hydroxyl) terminated, with isolated Fe(III)(O,OH,$H_2O$)$_6$ octahedra "adsorbed" in a tridentate fashion over a fraction of the Fe(III) vacancies on the C-cut surface. We speculate that the O-terminated regions of the surface from the CTR data fitting correspond to the O-terminations observed by Eggleston *et al.*[17] in their STM images and that the CTR-derived isolated Fe(III)(O,OH,$H_2O$)$_6$ octahedra correspond to the Fe-terminated regions suggested in the STM study. The isolated Fe(III)(O,OH,$H_2O$)$_6$ octahedra result in three "corner" sites per octahedron, which have one-coordinated oxygens exposed at the surface, rather than the two-coordinated oxygens that are present on the unrelaxed, unreconstructed, and unhydrated C-cut hematite surface presented in Figure 1. These singly coordinated oxygens are stronger Lewis bases (*i.e.*, they have higher electron density in the non-bonded oxygen orbitals) than their doubly coordinated counterparts, and thus are more reactive to Pb(II) than would be the case if the C-cut surface structure were a simple termination of the bulk.

The CTR results for the hydrated hematite C-cut differ from the CTR results for the C-cut surface of hydrated $\alpha$-$Al_2O_3$[5], which found the surface to be oxygen (or hydroxyl) terminated with no evidence for a partially occupied outer layer. Although significant relaxation of the outer three layers of $\alpha$-$Al_2O_3$ were observed, the surface oxygens were found to be dominantly two-coordinated as is the case for the simple termination of the unrelaxed bulk structure.

## Materials and Methods

Hematite (0001) and (1-102) substrates were grown as 300-400 Å thin films on oriented sapphire substrates (measuring 1 cm diam. x 0.1 cm thick) by oxygen-plasma-assisted multiple beam epitaxy methods[25,26] at Pacific Northwest National Laboratory. Multiple crystals of each cut were available and, within each orientation, were used interchangeably for EXAFS, reflectivity, and uptake measurements to facilitate experiments. Samples were washed in nitric acid, acetone, and methanol followed by multiple rinses with Milli-Q water prior to equilibration with aqueous solutions. Sample cleanliness and Pb(II) sorption density were characterized using x-ray photoelectron spectroscopy (XPS) (Surface Science S-Probe, monochromatic Al K$\alpha$ radiation). Sample surface planes were oriented at angles of 35° (survey scans) and 90° (detailed region scans) relative to the detector. Only Fe, O, and adventitious carbon were detected on the clean crystals. Pb(II) sorption density was calculated by taking the ratio of the reduced area[27] Pb 4f and Fe 3p lines and scaling it by the number of Fe atoms that should be observed from the sample per unit area, integrated over infinite depth in the bulk and assuming an electron escape depth of 18 Å. X-ray reflectivity profiles from samples were measured using a Philips MRD 4-circle diffractometer with a four-bounce Ge (220) monochromator; these indicated that the crystals had rms roughnesses of 1.0 to 1.3 Å (C cut) and 1.0 Å (R cut). Our previous synchrotron-based photoemission study of the reaction of water vapor with hematite single crystal surfaces showed that these surfaces readily react with water, resulting in a fully hydroxylated surface above a threshold pressure ($pH_2O$) of $\approx 3 \times 10^{-4}$ torr.[20]

Aqueous solutions were prepared from Milli-Q water, boiled with $N_2$ to remove $CO_2$ and subsequently cooled and maintained under $N_2$ atmosphere. Laboratory temperature was maintained at 23°C. A 250 μM $Pb(NO_3)_2$ solution was prepared at pH 7.01 and maintained under an atmosphere of pure $N_2$. pH adjustment was performed using $CO_2$-free NaOH, prepared using boiled $CO_2$-free water. Tabulated thermodynamic constants[28] predict that Pb(II) aqueous speciation under the experimental conditions should have been 94% $Pb^{2+}$(aq) or $Pb^{2+}\bullet NO_3^-$ complexes and approximately 6% should have been $PbOH^+$(aq). Multinuclear Pb(II) complexes should comprise less than 0.1% of dissolved Pb(II). No Pb(II) oxides, hydroxides, or basic Pb(II) nitrates should have precipitated under these solution conditions. Furthermore, Pb(II)-reacted crystals showed no detectable nitrate or carbonate, as determined by XPS.

Fluorescence-yield Pb $L_{III}$ EXAFS data were collected at SSRL beamline 6-2 using a 13-element Ge detector array and a grazing-incidence apparatus, which allows positioning of the sample in the three Eulerian angles $\theta$, $\chi$, and $\phi$ and in z.[29] The angle of incidence of x-rays on the crystal surfaces was set to 0.14° (which is below the critical angle for total external reflection of hematite) during EXAFS data collection. X-ray optics included a Pt-coated focusing mirror located upstream of a Si(111) double-crystal monochromator. Absorption of x-rays at the Pt $L_{II}$-edge prevented Pb $L_{III}$-EXAFS data collection above k = 8 Å$^{-1}$. Tantalum slits were used to define 50 μm vertical apertures upstream of the experiment. Hematite crystals were loaded into a Teflon sample cell[8] at the beam line and covered with a 1.5 μm-thick polypropylene membrane. The cell was purged with dry $N_2$ and filled with the Pb(II) solution, which was then allowed to react with the hematite crystals for 90 to 120 minutes. Excess solution was withdrawn from the cell, and it was placed under a slight negative pressure to maintain a thin film of solution (≈ 1μm thick) above the crystal. The water layer thus achieved was sufficiently thick to ensure that its bulk properties were not perturbed by the oxide or polypropylene surfaces. A water-saturated $N_2$ atmosphere was maintained above the cell to prevent the solution film from drying, and to minimize $CO_2$ diffusion through the polypropylene membrane. Pb(II) surface coverage on the crystals was estimated in parallel experiments in which crystals were reacted for 90 to 120 min. in unstirred solutions maintained in $N_2$-purged, sealed 15 mL HDPE centrifuge tubes.

Unsmoothed, background-subtracted, $k^3$-weighted EXAFS data were fit in k-space by a non-linear least squares procedure using the EXAFSPAK software.[30] Oxidation of Pb(II) to Pb(IV) was observed to occur after about 8 hr of beam exposure of the hematite C-cut/Pb(II) sorption sample. This reaction was significantly slower on the R-cut surface. Only the first 5 hours and 8 hours of EXAFS data for the C- and R-cut samples, respectively, were averaged for data analysis because of Pb oxidation. Phase and amplitude functions used to fit these data were extracted from well-characterized, crystalline model compounds and FEFF 6 calculations[31] as described previously.[32] Interatomic distances involving Pb were found to be accurate to ±0.03Å for first-neighbor oxygens and ±0.04Å for Pb and Fe second neighbors. Coordination numbers (CN) are accurate to ± 20% for closest 1st-shell oxygens.[32] Pb-O $\sigma^2$ values varied to 0.01 Å$^2$ during the fits and were subsequently fixed at this value to reduce the degrees of freedom in the fits and facilitate comparison of the EXAFS. A similar procedure was used for powder sorption samples.[33,34] The presence of $Pb^{2+}$(aq) in the solution film overlying the sample necessitated addition of an oxygen shell at 2.51 Å[32] to spectral fits, for which only CN was allowed to vary. Reasonable fits to the spectra could not be obtained without inclusion of this shell. The CN for this shell was found to be poorly constrained in the C-cut sample and was subsequently set to be equivalent to the value obtained for the R-cut sample. A single value of $\Delta E_O$ was applied to all shells in each sample, and was varied during fitting. $S_0^2$ was fixed at 0.843 in all fits based on prior results.[33] Fit results are presented in Table 1 and discussed below. The polarization dependence of X-ray absorption (*i.e.*, relative to the crystallographic orientation of the surface) is very weak at the $L_{III}$ edge[35]. For this reason and because of the high degree of disorder in the lead coordination shell[32], the EXAFS and XANES spectra should be largely unaffected by the orientation of the sample relative to the s-polarized incoming x-ray beam, and we did not attempt to explicitly account for polarization effects.

**Table 1.** XPS and EXAFS results.

| | XPS | | EXAFS | | | |
|---|---|---|---|---|---|---|
| Sample | $\Gamma$ (atoms /nm$^2$) | | O | Oaq†† | Fe | Pb |
| Pb(II)/(0001) (C-cut) | 8.3 (1.0) | CN | 2.5 (.1) | 0.8 | 0.4 (.2) | 2.8 (.6) |
| | | R(Å) | 2.24 (.01) | 2.51 | 3.81 (.06) | 3.62 (.03) |
| | | $\sigma^2$ (Å$^2$) | 0.01 | 0.01 | 0.01 | 0.01 |
| Pb(II)/(1-102) (R-cut) | 7.2 (0.9) | CN | 2.0 (.2) | 0.8 (.4) | 0.4 - 0.6 | 2.9 (.6) |
| | | R(Å) | 2.280 (.007) | 2.51 | 3.34 – 3.86* | 3.69 (.04) |
| | | $\sigma^2$ (Å$^2$) | 0.01 | 0.01 | 0.01 | 0.01 |
| Pb(II)/Hematite powder, pH 7† | 1.2 - 6.0 | CN | 2.2 (.1) | -- | 0.5 (.1) | -- |
| | | R(Å) | 2.28 (.01) | -- | 3.28 (.02) | -- |
| | | $\sigma^2$ (Å$^2$) | 0.01 | -- | 0.01 | -- |

$\Gamma$ = sorption density, CN = coordination number, R = interatomic distance, $\sigma^2$ = Debye-Waller factor. Estimated standard deviations are given in parentheses. †From Bargar *et al.*[33]. ††This shell accounts for aqueous and outer-sphere species. *See text for discussion.

## Results and Discussion

**Pb(II) uptake on Hematite (0001) and (1-102).** The Pb(II) sorption densities on hematite C and R cut crystals measured by XPS were 8.3 and 7.2 Pb atoms/nm$^2$ (Table 1, Figure 2.). In comparison, the densities of Fe atoms in the top-most metal-bearing layers of the ideal oxygen-terminated C and R cut hematite surfaces depicted in Figure 1 are 9.1 and 10 sites/nm$^2$. If one assumes a monolayer of Pb(II) to be equivalent to the Fe surface atom densities, then the measured Pb(II) sorption densities suggest > 70% effective monolayer coverage of Pb(II) on the hematite surfaces. In principle, surface-bound Pb(II) can occur on hematite as islands (*e.g.,* oligmeric complexes) and/or as small (*e.g.*, monomeric) complexes evenly distributed across hematite surfaces. These modes of occurrence can not be readily distinguished from the XPS data set because of uncertainty regarding the extent and manner of changes of the in-plane interfacial Pb(II) distribution upon removal of the crystals from solution and placement into high-vacuum conditions for XPS analyses.

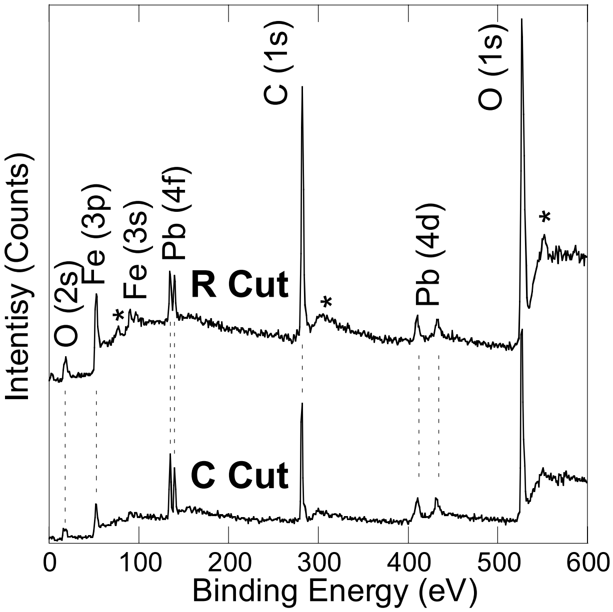

**Figure 2.** XPS survey scans of Pb(II)-reacted R and C-cut samples. * Denotes plasmon loss lines.

**XANES Results.** Pb $L_{III}$-edge XANES spectra are shown in Figure 3. Pb(II) XANES are highly sensitive to the 1st-shell coordination geometry.[32] The Pb(II)/hematite single crystal XANES spectra

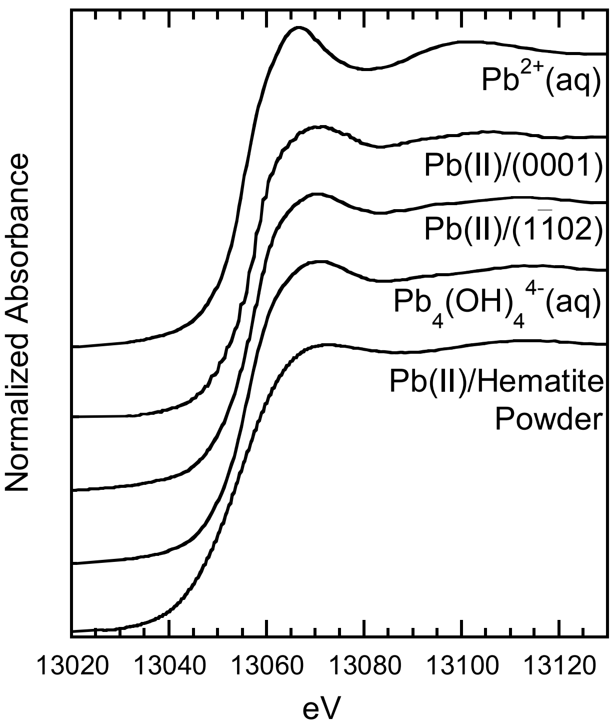

**Figure 3.** Normalized XANES spectra of Pb(II) adsorbed on hematite C and R surfaces, compared to selected model compounds. The spectrum for Pb(II)/hematite powder is at pH 7 corresponds to the reference spectrum in Table 1 and was measured at lower spectrometer resolution than the other spectra.

are identical to those for Pb(II) adsorbed on hematite powders in an inner-sphere mode and differ from the XANES for $Pb^{2+}$(aq). These observations indicate that a change in Pb(II) local coordination environment occurred upon adsorption of $Pb^{2+}$(aq) onto hematite and suggest the formation of inner-sphere complexes, *i.e.*, the direct bonding of Pb(II) to (hydr)oxo surface groups. The Pb(II)/hematite single crystal XANES spectra are also generally similar to that for $Pb_4(OH)_4^{4-}$(aq) (Figure 3). This similarity was noted in previous studies of Pb(II)/hematite powders[33] and was interpreted as indicating that Pb(II) is bonded to oxo and/or hydroxo ligands (which could include hematite surface oxygens) arranged around Pb(II) in a distorted trigonal pyramidal geometry.[32,33]

The Pb(II)/hematite single crystal XANES are distinctly different from XANES for $PbCO_3$, $Pb_3(OH)_2CO_3$, and basic Pb(II) nitrate (*cf.* references 32-34, 36, and 37), which are the solid phases that can be formed in bulk solution if carbonate is not excluded or if the Pb(II) concentration exceeds about

1 mM[32], and are different from the XANES of different forms of PbO[32]. The precipitation of these solid phases can thus be ruled out.

**EXAFS Results: Mode of Sorption of Pb(II) on Hematite (0001) and (1-102)** Pb $L_{III}$-edge EXAFS spectra and the corresponding Fourier Transforms (FTs) are shown in Figure 4. Throughout this paper, FT peak distances are reported in units of Å, uncorrected for phase shift (*i.e.*, R - ΔR). In contrast, when referring to neighboring atoms around Pb(II), we report the EXAFS-derived distances, which include correction for phase shift (ΔR). The most intense feature in all spectra is a (damped) sinusoidal curve from oxygen backscattering, for which the characteristic FT frequency occurs at *ca* 1.4 Å. Fits to the spectra indicate the primary contribution to this FT peak is an oxygen shell at 2.24 to 2.28 Å (Table 1). The FT peak also contains minor amplitude contributions from $Pb^{2+}$(aq) in the overlying aqueous film, which was quantitatively taken into account during the EXAFS fitting.

The coordination chemistry of lead oxides and oxosalts, particularly with respect to the first shell coordination geometry, was reviewed extensively in Bargar *et al.* (1997)[32]. In general, Pb(II) coordination compounds show a large range of Pb-O distances, with 2.24 Å being on the shortest end of the range. Previously reported Pb(II) species exhibiting Pb-O distances as short as 2.24 Å (and which could be present in the samples) are: (i) Pb(II) bonded to hematite surfaces as an monomeric inner-sphere complex (for which $R_{Pb\text{-}O}$ = 2.25 to 2.33 Å[9,33,34]), (ii) the aqueous $Pb_4(OH)_4^{4-}$ complex (present as an outer-sphere species), or (iii) solid-phase PbO, basic Pb(II)-nitrate, or basic Pb(II)-carbonate. The latter compounds can be ruled out because their EXAFS spectra[32,33,34,36,37] differ substantially from the Pb(II)/hematite single crystal EXAFS shown in Figure 4. The $Pb_4(OH)_4^{4-}$(aq) complex can also be ruled out based on the differences between its EXAFS and those for the sorption samples (Figure 4). Thus, by comparison to previously described compounds, the EXAFS-derived Pb-O bond distances imply that Pb(II) is bonded to hematite as inner-sphere complexes in the present samples.

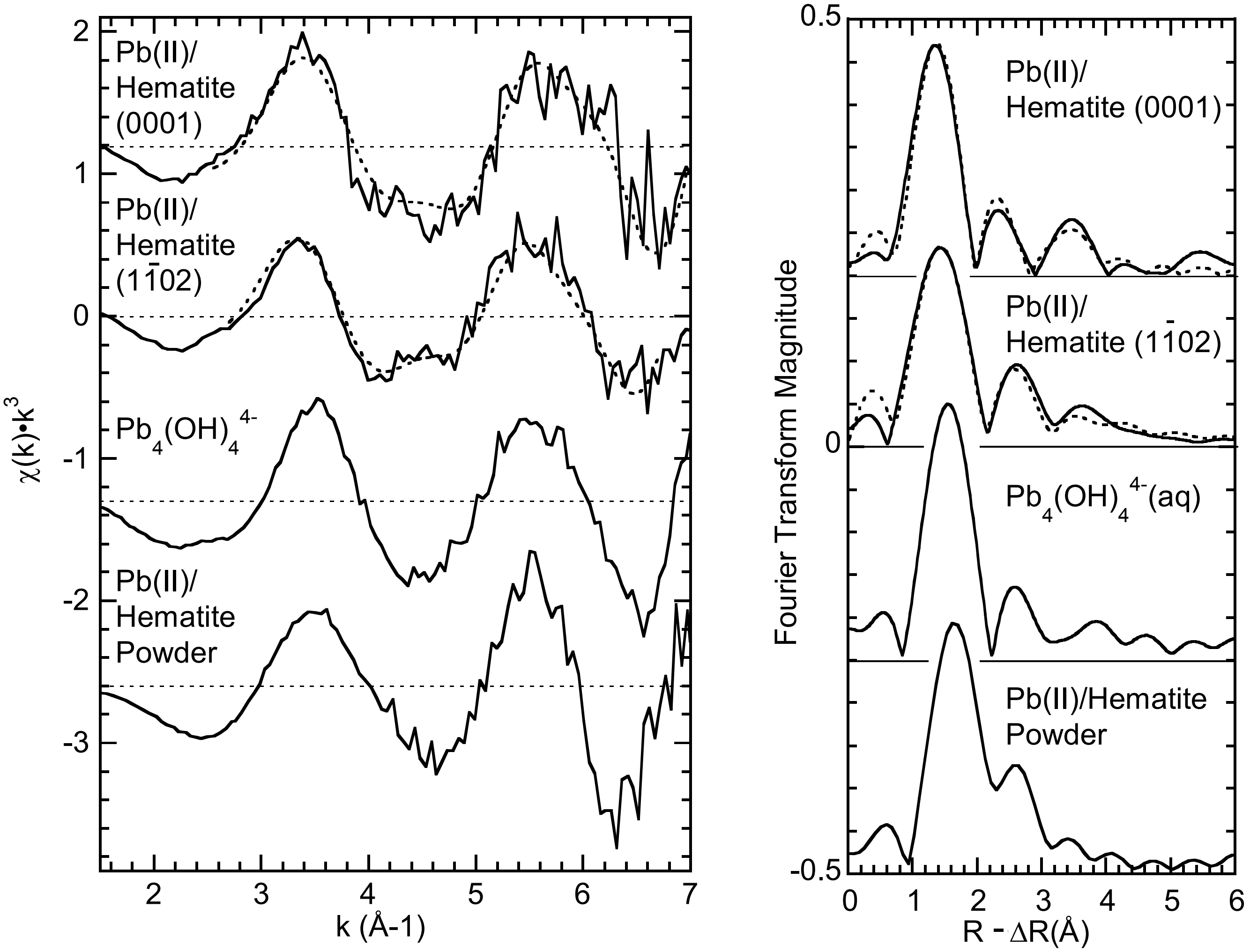

**Figure 4.** EXAFS spectra and corresponding Fourier Transforms (FTs) for Pb(II) adsorbed on hematite C- and R-cut surfaces, $Pb_4(OH)_4^{4-}$ (aq), and Pb(II) adsorbed on hematite powders at pH 7[33]. FTs are uncorrected for phase shift. Dotted lines are fits to sample spectra.

Pb(II) coordination complexes that display the short 2.20 – 2.30 Å Pb-O bond length typically exhibit a highly distorted trigonal pyramidal first-shell coordination geometry for Pb(II), with 3 oxygens/hydroxyls forming the triangular base and with an electron lone pair defining the pyramid apex[32]. Typically, it is not possible to observe all 3 first-shell oxygens using EXAFS because the asymmetry of the first oxygen shell causes destructive interference of the oxygen backscattering, which is not adequately described by harmonic Debye-Waller amplitude-reduction terms[32]. First-shell CNs of 2 to 2.5 were obtained in the present study and are comparable to previous investigations using powder hematite samples.[33] Some of the apparent Pb-O amplitude loss in the present study can be attributed to the presence of a small amount of aqueous $Pb^{2+}$, which dilutes the signal from surface-bound lead by 10% to 15%. To further account for missing amplitude, we attempted fits in which the oxygen shell Debye-Waller term was expanded to include the 3rd-order cumulant.[38] These fits yielded approximately the same CNs as obtained with the 2nd-order Debye-Waller term. Furthermore, 3rd-order cumulant fits to room-temperature model compounds (orthorhombic PbO, $PbNO_3$) could not account for the "missing" oxygen amplitude in the EXAFS. We conclude that the cumulant expansion approach does not adequately account for the bond-length asymmetry in Pb-O shell. This inadequacy has been observed in previous EXAFS studies of metal ions in high-temperature superconductors and silicate liquids, where anharmonicity is severe.[39,40]

The sample spectra for Pb(II) on both the R-cut and C-cut surfaces also contain backscattering from 2nd-neighbor atoms, seen as peaks at about 2.5 and 3.5 Å in the FTs. Multiple scattering processes are not expected to generate FT peaks at these distances, given the low symmetry of the Pb(II) environment.[32] Nearest-neighbor oxygen shells were initially fit and subtracted from the EXAFS data to facilitate analysis of the 2nd-neighbor shells. The addition of a single shell of Pb(II) neighbors at about 3.65 Å to the fits accounted for 70 to 80% of the 2nd-shell amplitude in both samples. The backscattering contributions from a single shell of Pb can account for both of the 2nd-neighbor peaks in the FT because the backscattering amplitude function for Pb-Pb pairs goes through a deep minimum at ~5 $Å^{-1}$, while the backscattering phase function changes rapidly. In comparison, addition of single Fe shell to the fits provided $chi^2$ fit values approximately 1.3 to 1.7 times larger than obtained with Pb and generally poor reproductions of the spectra. Physically realistic, acceptable fits were not obtained using two Fe shells (absent of Pb). However, inclusion of an Fe shell, in addition to a second Pb(II) shell, in the fits of the EXAFS caused the $chi^2$ fit value to decrease by factors of 2 (C-cut) to 3 (R-cut) in the residual spectra, obtaining the results shown in Figure 4 and Table 1.

The EXAFS-derived Pb-Pb distance is in the range 3.62 to 3.69 Å for both the hematite C-cut and R-cut surfaces. Since the sample EXAFS are inconsistent with solid phase precipitates, it is appropriate to interpret the Pb second neighbors in the context of adsorbed oligomeric Pb(II) complexes. The 3.62 to 3.68 Å Pb-Pb distances are similar to those observed in $Pb_4(OH)_4^{4-}$ complexes (3.76 Å [32,41,42]) and those observed in PbO (3.66 Å [43]), suggesting that the adsorbed complexes have a local structure comparable to these species. In $Pb_4(OH)_4^{4-}$, Pb(II) occurs in tetrameric complexes, in which each Pb shares polyhedral edges with 3 Pb neighbors. In PbO, each Pb shares polyhedral edges with 4 Pb neighbors in a sheet-like structure. The EXAFS-derived Pb CNs of 2.8 to 2.9 Pb second neighbors are consistent with the tetrameric structure as well as with a PbO-like structure of small size (*i.e.*, missing Pb atoms at the edges of the structure). The overall picture that arises is one of oligomeric complexes in which Pb atoms share polyhedral edges with 3 other Pb atoms.

The EXAFS-derived Pb-Fe distances lie in the range of 3.34 to 3.92 Å. Both distances have been previously observed for Pb(II) adsorbed on hematite powders.[33] The 3.34 Å distance indicates edge-sharing between Pb(II) polyhedra and $FeO_6$ octahedra, whereas the 3.9 Å distance indicates corner-sharing linkages. In the case of Pb(II) sorbed on R-cut hematite, the quality of the data did not permit distinction between these two distances. The presence of Fe neighbors at these distances is consistent with direct bonding of Pb(II) to (hydr-)oxo groups on both C- and R-cut hematite surfaces.

### Fundamental Controls on Hematite Surface Reactivity.

The conclusion that Pb(II) bonds to the hematite C-cut surface suggests that either $\equiv Fe_2O$ surface sites are capable of coordinating Pb(II), in general support of the model predictions by Ostergren *et al.*[9], or that there are additional surface oxygen functional groups present on the hematite C-cut surface as compared to the $\alpha$-$Al_2O_3$ C-cut surface. Based on the recent surface structural evidence discussed in the introduction section, we propose that the predominant reason for the finding of inner-sphere Pb(II) surface complexes on the hematite C-cut surface is likely due to the presence of "adsorbed"

$Fe(III)(O,OH,H_2O)_6$ species, which provide single (and triple) coordinated surface oxygens exposed at the surface. These "adsorbed $Fe(III)(O,OH,H_2O)_6$ species" would provide a large number of sites available for Pb(II) to bind either as bidentate edge-sharing or monodentate corner-sharing complexes, as suggested by the GI-EXAFS results. This results supports both recent STM results[17] and CTR work[18,19] on the hydrated hematite C-cut surface.

Oligomeric Pb(II) complexes were previously not observed on hematite powders[33] at Pb(II) sorption densities comparable to those obtained in the present study (Table 1). Oligomeric complexes have been reported to exist as a minor species on $Al_2O_3$ powders.[32] In comparison, the present study finds that the majority of Pb(II) on hematite R- and C-cut surfaces occurs as oligomeric complexes. The solution conditions of the present study mirror those of the previous studies[33]. Thus, the primary differences between the present and previous studies are: (a) the extreme flatness of the single-crystal surfaces in comparison to the rough surfaces present on powders, and (b) the use of only two crystallographic orientations in the present study as opposed to a multitude of orientations presented to solution by the powders. While we can not eliminate either of these potential explanations, there are several reasons to favor explanation (a). The present EXAFS and XPS results suggest that Pb(II) has a similar mode of occurrence on the structurally distinct hematite C- and R-cut surfaces. Furthermore, the C-cut surface is a dominant growth face on particulate hematite and is expected to have been well represented in the previous powder studies. In comparison, the density of step edges is thought to be higher on powders than on the single crystals of the present study. Thus, the presence of oligomeric Pb(II) complexes in the present study should correlate inversely with the density of step edges. Based on this analysis, we tentatively conclude that oligomeric Pb(II) complexes represent the preferred species on a flat surface where hematite step edge sites are scarce.

## Concluding Remarks

Aqueous Pb(II) adsorbs on hematite C- and R-cut surfaces as inner-sphere surface complexes. Pb(II) also sorbs in an inner-sphere fashion on the R-cut surface of $\alpha$-$Al_2O_3$,[7,8], which has about equal proportions of one-, two-, and three-coordinated oxygens.[6] This behavior is different than observed in previous studies[7,8] using the $\alpha$-$Al_2O_3$ C-cut surface, in which Pb(II) was found to adsorb in an ordered, outer-sphere fashion. The predominant Pb(II) species sorbed on hematite surfaces under the experimental conditions used in the present study is an oligomeric Pb(II) adsorption complex. XANES and EXAFS suggest the local structure of adsorbed Pb(II) to be a distorted trigonal pyramid of oxide and/or hydroxide ligands, some of which are part of the hematite surface. These results suggest that $\equiv Fe_2O$ as well as $\equiv FeOH$, and $\equiv Fe_3O$ surface sites can coordinate Pb(II), in general support of the hematite surface bond-valence model proposed by Ostergren *et al.*[9] and consistent with recent CTR results for the hydrated hematite surface in contact with bulk water, which revealed the presence of isolated $Fe(O,OH,H_2O)_6$ octahedra with three highly reactive one-coordinated oxygens per octahedron.[18,19] A more complete understanding of potential differences in the reactivity of the C- and R-cut surfaces of hydrated hematite will be provided by CTR data for R-cut hematite, which are currently being analyzed.[44]

ACKNOWLEDGMENTS. We dedicate this paper to Steven N. Towle, our research partner in earlier GI-EXAFS investigations of the structures of Pb(II) and Co(II) adsorbate complexes at $Al_2O_3$ and $TiO_2$ surfaces. Steve died in a tragic skiing accident this summer at the age of 35. We will deeply miss him. We thank Alexis Templeton and Daniel Grolimund for their helpful comments on earlier drafts of this paper. This work was supported by DOE Grant DE-FG03-93ER14347-A008 (Brown) and by NSF-CRAEMS Grant CHE-0089215 (Brown). SSRL is operated by Stanford University on behalf of the U.S. Department of Energy, Office of Basic Energy Sciences. In addition to support from the Office of Basic Energy Sciences, SSRL is supported by the Department of Energy, Office of Biological and

Environmental Research, and by the National Institutes of Health, National Center for Research Resources, Biomedical Technology Program.

## REFERENCES

(1) Brown, G. E., Jr.; Henrich, V. E.; Casey, W. H.; Clark, D. L.; Eggleston, C.; Felmy, A.; Goodman, D. W.; Grätzel, M.; Maciel, G.; McCarthy, M. I.; Nealson, K.; Sverjensky, D. A.; Toney, M. F.; Zachara, J. M. *Chem. Rev*. **1999***, 99*, 77-174.

(2) Nelson, Y. M.; Lion, L. W.; Shuler, M. L.; Ghiorse, W. C. *Limnology* **1999**, *44*, 1715-1729.

(3) Templeton, A. S.; Trainor, T. P.; Traina, S. J.; Spormann, A. M.; Brown, G. E., Jr. *Proc. Natl. Acad. Sci.* **2001**, *98*, 11897-11902.

(4) Brown, G. E., Jr.; Parks, G. A. *Int. Geol. Rev.* **2001**, *43*, 963-1073.

(5) Eng, P. J.; Trainor, T. P.; Brown, G. E., Jr.; Waychunas, G. A.; Newville, M.; Sutton, S. R.; Rivers, M. L. *Science* **2000**, *288*, 1029-1033.

(6) Trainor, T. P.; Eng, P. J.; Brown, G. E., Jr.; Robinson, I. K.; De Santis, M. *Surf. Sci.* **2002**, *496*, 238-250.

(7) Bargar, J. R.; Towle, S. N.; Brown, G. E., Jr.; Parks, G. A. *Geochim. Cosmochim. Acta* **1996**, *60*, 3541-3547.

(8) Bargar, J. R.; Towle, S. N.; Brown, G. E., Jr.; Parks, G. A. *J. Colloid Interface Sci.* **1997**, *185*, 473-492.

(9) Ostergren, J. D.; Trainor, T. P.; Bargar, J. R.; Brown, G. E., Jr.; Parks, G. A. *J. Colloid Interface Sci.* **2000**, *225*, 466-482.

(10) Hiemstra, T.; Wit, J. C. M. D.; Riemsdijk, W. H. V. *J. Colloid Interface Sci.* **1989**, *133*, 91-104.

(11) Hiemstra, T.; Venema, P.; Van Riemsdijk, W. H. *J. Colloid Interface Sci.* **1996**, *184*, 680-692.

(12) Hiemstra, T.; Van Riemsdijk, W. H. *J. Colloid Interface Sci.* **1996**, *179*, 488-508.

(13) Towle, S. N.; Parks, G. A.; Brown, G. E., Jr. *J. Colloid Interface Sci.* **1999**, *217*, 299-311.

(14) Towle, S. N.; Bargar, J. R.; Brown, G. E., Jr.; Parks, G. A. *J. Colloid Interface Sci.* **1999**, *217*, 312-321.

(15) Nriagu, J. O. (ed.) *The Biogeochemistry of Lead in the Environment.* Elsevier/North Holland Biomedical Press, New York, 1978.

(16) Brown, G. E., Jr.; Sturchio, N. C. *Rev. Mineral. Geochem*. **2002**, *49*, 1-115.

(17) Eggleston, C. M.; Stack, A. G.; Rosso, K. M.; Higgins, S. R.; Bice, A. M.; Boese, S. W.; Pribyl, R. D.; Nichols, J. J. *Geochim. Cosmochim. Acta* **2003**, *67*, 985-1000.

(18) Trainor, T. P.; Eng, P.; Brown, G. E., Jr.; Waychunas, G. A.; Newville, M.; Sutton, S. R.; Rivers, M. L. *2001 Activity Report,* Advanced Photon Source, 2002.

(19) Trainor, T. P., Chaka, A.M., Eng, P.J. Newville, M, Waychunas, G.A., Catalano, J.G., Brown. G.E., Jr., **2003** (Submitted).

(20) Liu, P.; Kendelewicz, T.; Brown, G. E., Jr.; Nelson, E. J.; Chambers, S. A. *Surf. Sci.* **1998**, *417*, 53-65.

(21) Condon, N. G.; Leibsle, F. M.; Lennie, A. R.; Murray, P. W.; Parker, T. M.; Vaughan, D. J.; Thornton, G. *Surf. Sci.* **1998**, *397*, 278-287.

(22) Wang, X.-G.; Weiss, W.; Shaikhutdinov, Sh. K.; Ritter, M.; Petersen, M.; Wagner, F.; Schlögl, R.; Scheffler, M. *Phys. Rev. Lett.* **1998**, *81*, 1038-1041.

(23) Kettler, G.; Weiss, W.; Ranke, W. *Surf. Rev. Lett.* **2001**, *8*, 661-683.

(24) Shaikhutdinov, Sh. K.; Weiss, W. *Surf. Sci.* **1999**, *432*, L627-L634.

(25) Kim, Y. J.; Gao, Y.; Chambers, S. A. *Surf. Sci.* **1997**, *371*, 358-370.

(26) Chambers, S. A. *Surf. Sci. Rep.* **2000**, *39*, 105-180.

(27) Spruytte, S.; Coldren, C.; Harris, J.; Pantelidis, D.; Lee, H.-J.; Bravman, J.; Kelly, M. *J. Vac Sci. Technol.* **2001**, *A 19*, 603-608.

(28) Baes, C. F.; Mesmer, R. E. *The Hydrolysis of Cations*; John Wiley & Sons: New York, 1976.

(29) Yu, E. Y.; Penner-Hahn, J. E.; Yocum, C. F.; Mayer, R. H.; Pickering, I. J. *Rev. Sci. Instrum.* **1996**, *67*, 1 - 4.

(30) George, G. N. *EXAFSPAK*; Stanford Synchrotron Radiation Laboratory: Stanford, 1993.

(31) Rehr, J. J.; Albers, R. C. *Phys. Rev. B* **1990**, *41*, 8139-8149.

(32) Bargar, J. R.; Brown, G. E., Jr.; Parks, G. A. *Geochim. Cosmochim. Acta* **1997**, *61*, 2617-2637.

(33) Bargar, J. R.; Brown, G. E., Jr.; Parks, G. A. *Geochim. Cosmochim. Acta* **1997**, *61*, 2639-2652.

(34) Bargar, J. R.; Brown, G. E., Jr.; Parks, G. A. *Geochim. Cosmochim. Acta* **1998**, *62*, 193-207.

(35) Citrin, P.H. *Phys. Rev. B* **1985**, *31*, 700-721.

(36) Ostergren, J. D.; Brown, G. E., Jr.; Parks, G. A.; Tingle, T.N. *Environ. Sci. Technol.* **1999**, *33*, 1627-1636.

(37) Ostergren, J. D.; Brown, G. E., Jr.; Parks, G. A.; Persson, P. *J Colloid Interface Sci.* **2000**, *225*, 483-493.

(38) Crozier, E. D.; Rehr, J. J.; Ingalls, R. In: *X-ray Absorption. Principles, Applications, Techniques of EXAFS, SEXAFS and XANES*, Chemical Analysis, **92**, D.C. Koningsberger, R. Prins, eds., pp. 373-442, John Wiley & Sons, New York, 1988.

(39) Mustre de Leon, J.; Conradson, S. D.; Bishop, A. R.; Raistric, I.; Batistic, I.; Jackson, W. E.; Brown, G. E., Jr.; Waychunas, G. A. In: *XAFS VI, Sixth Internat. Conf. on X-ray Absorption Fine Structure*, ed. S.S. Hasnain, Ellis Horwood Ltd, Publishers, p. 54-57, 1991.

(40) Jackson, W. E.; Brown, G. E., Jr.; Waychunas, G. A.; Mustre de Leon, J.; Conradson, S. D.; Combes, J.-M. *Science* **1993**, *262*, 229-233.

(41) Hong, S.; Olin, Å. *Acta Chem. Scand*. **1974**, A28, 233 - 238.

(42) Hong, S.; Olin, Å. *Acta Chem. Scand.* **1973**, *27*, 2309 – 2320

(43) Boher, P., Garnier, P. Gavarri, J.R., and Hewat, A.W. , *J. Solid State Chem.* **1985,** *57*, 343-350.

(44) Trainor, T. P. *et al*. **2003** (in preparation)